Adsorption (2008) 14: 223–239
DOI 10.1007/s10450-007-9079-4

Nonlinear FR-ZLC method for investigation of adsorption equilibrium and kinetics

Menka Petkovska

Received: 27 April 2007 / Revised: 25 September 2007 / Accepted: 30 October 2007 / Published online: 21 November 2007

Abstract A new method for investigation of adsorption equilibrium and kinetics, named Nonlinear Frequency Response-Zero Length Column (NFR-ZLC) method, is introduced. It combines the advantages of the Nonlinear FR method (the potential to identify a model corresponding to the most probable kinetic mechanism and to estimate the equilibrium and kinetic parameters of the identified model) and of the ZLC method (the potential to derive direct information about the processes on the particle level, by eliminating the influence of the adsorber). The frequency response functions of a ZLC system, up to the third order, and for three simple kinetic mechanisms (film resistance control, micropore diffusion control and pore-surface diffusion control) are derived and simulated. The procedure for estimation of the equilibrium and kinetic parameters is defined and illustrated based on numerical simulations.

Keywords Nonlinear FR · ZLC · Equilibrium · Kinetics · Mechanism identification · Parameter estimation

Nomenclature

A	input amplitude
$\tilde{a}_c$	first order coefficient of the Taylor series expansion of the isotherm relation $q = \varphi(c)$
$\tilde{a}_q$	first order coefficient of the Taylor series expansion of the isotherm relation $c = \Gamma(q)$
B	amplitude of the output harmonic
$\tilde{b}_c$	second order coefficient of the Taylor series expansion of the isotherm relation $q = \varphi(c)$
$\tilde{b}_q$	second order coefficient of the Taylor series expansion of the isotherm relation $c = \Gamma(q)$
C	concentration in the fluid phase, mol/m^3
C_i	concentration in the fluid phase within the particle pores (pore-surface diffusion model), mol/m^3
c	nondimensional concentration in the fluid phase
c_i	nondimensional concentration in the fluid phase within the particle pores (pore-surface diffusion model)
$\tilde{c}_c$	third order coefficient of the Taylor series expansion of the isotherm relation $q = \varphi(c)$
$\tilde{c}_q$	third order coefficient of the Taylor series expansion of the isotherm relation $c = \Gamma(q)$
D_{eff}	effective diffusion coefficient, m^2/s
D_p	pore diffusion coefficient, m^2/s
D_s	surface diffusion coefficient, m^2/s
D_μ	micropore diffusion coefficient, m^2/s
F	FRF on the particle level
G	FRF on the column level
k_m	mass transfer coefficient, 1/s
Q	concentration in the adsorbent particle, mol/m^3
q	nondimensional concentration in the adsorbent particle
Q_i	concentration in the solid phase (pore-surface diffusion model), mol/m^3
q_i	nondimensional concentration in the solid phase (pore-surface diffusion model)
R	particle half-dimension, m
R_μ	microparticle half-dimension, m
r	particle spatial coordinate, m
r_μ	microparticle spatial coordinate, m
t	time, s
V	volume of the ZLC bed, m^3
$\dot{V}$	volumetric flow-rate, m^3/s
W	function defined in (49)

M. Petkovska (✉)
Department of Chemical Engineering, Faculty of Technology and Metallurgy, University of Belgrade, Karnegijeva 4,
11000 Belgrade, Serbia
e-mail: menka@tmf.bg.ac.yu

X input, general, frequency domain
x input, general, time domain
Y output, general, frequency domain
y output, general, time domain
Z functions defined in (43)–(45)

Greek letters

β time constant corresponding to accumulation in the particles of the ZLC, s
Γ adsorption isotherm function (φ^{-1})
γ time constant corresponding to accumulation in the interstitial fluid of the ZLC, s
ε bed porosity
ε_p particle porosity
ε'_p modified particle porosity
φ adsorption isotherm function, phase (rad)
σ shape factor
τ time constant, s
ω frequency, rad/s
ω^* complex parameter defined in (65) and (70)

Subscripts

1 first order
2 second order
3 third order
I first harmonic
II second harmonic
III third harmonic
F film resistance model
M micropore diffusion model
PS pore-surface diffusion model
s corresponding to stationary state

Abbreviations

FR frequency response
FRF frequency response function
ZLC zero length column
$\langle\,\rangle$ mean value

1 Introduction

Like other heterogeneous solid-fluid systems, adsorption systems generally involve a number of interacting phenomena and processes. For their proper design, the knowledge of both equilibrium and kinetics is essential. In spite of a number of existing experimental techniques for measuring adsorption equilibrium (Rouquerol et al. 1999; Guiochon et al. 1994; Do 1998; Seidel-Morgenstern 2004) and kinetics (Kärger and Ruthven 1992; Do 1998), there is still a need for developing new methods.

The new method for investigation of adsorption equilibrium and kinetics, presented in this paper, is essentially a combination of two existing macroscopic methods: the Nonlinear Frequency Response (NFR) and the Zero Length Column (ZLC) method.

The zero length column (ZLC) method is a well known, essentially chromatographic technique. It was originally developed by Eić and Ruthven (1988) to measure intracrystalline diffusivities in zeolite crystals. Since then, the application of the ZLC method has been extended to kinetic investigation of various adsorption systems with different mechanisms (Ruthven and Brandani 2000; Eić et al. 2002; Cherntongchai and Brandani 2003; Barcia et al. 2005; Dunnewijk et al. 2006; Vinh-Thang et al. 2006), and also to equilibrium measurements (Brandani et al., 2003a, 2003b). Although isothermal and linear systems are usually considered, nonisothermal and nonlinear cases have also been investigated to some extent (Brandani 1998; Brandani et al. 1998, 2000).

The basic advantage of the ZLC method lies in the fact that a very shallow ("zero-length") column is used in the experiments, in order to eliminate the influence of the axial concentration gradient and axial dispersion. In the classical ZLC method an inert stream is passed through a shallow bed of adsorbent particles previously saturated by a sorbate, causing its desorption. The kinetic data are obtained by fitting the time dependent effluent concentration to the solution of a previously assumed mathematical model. Using the "zero-length" column justifies using the mathematical model on the particle scale, by neglecting the influence of the column.

On the other hand, the nonlinear frequency response method (NFR) is a rather new method for investigation of adsorption systems. It has been developed as an extension of the classical frequency response (FR) method, by applying the mathematical tools of Volterra series, generalized Fourier transform and the concept of higher order frequency response functions (FRFs).

Frequency response (FR) is a quasi-stationary response of a system to a periodic input change around a steady-state value. Its application for investigation of adsorption kinetics originates from 1963 (Naphtali and Polinski 1963), and since then it has been used by a number of research groups. A comprehensive overview of these investigations can be found in (Rees and Song 2000; Petkovska 2005b).

In all these investigations, the generally nonlinear adsorption systems are treated by the linear FR technique, which is justified by using very small input amplitudes (e.g. ∼1%, Song and Rees 1996 or 2%, Grenier et al. 1999 for reservoir volume modulations and <5% for pressure and concentration variations, Wang et al. 2003; Wang and LeVan 2007). As a result, a single frequency transfer function is obtained and its characteristics are used for estimation of the kinetic parameters. One of the main drawbacks of the classical, linear frequency response method is that a number of different

kinetic mechanisms result with the same shape of the linear FR characteristic functions (e.g. the micropore, pore or pore-surface diffusion mechanisms, Park et al. 1998). In that way, the method is reduced to estimation of kinetic parameters of a previously assumed model.

By using larger amplitudes of the input modulation function, the nonlinear behaviour of the system becomes visible. The nonlinear FR is obtained in the form of a complex periodic function which, in addition to the basic harmonic, generally contains a nonperiodic (DC) term and a number of higher harmonics:

$$x = A\cos(\omega t) \Rightarrow$$
$$y = y_{DC} + B_I\cos(\omega t + \varphi_I) + B_{II}\cos(2\omega t + \varphi_{II}) + B_{III}\cos(3\omega t + \varphi_{III}) + \cdots \quad (1)$$

The concept of higher order FRFs (Weiner and Spina 1980) is practically based on replacing the nonlinear model of the system by a set of FRFs of the first, second, third, etc. order. While the first order function is identical to the one resulting from the linear FR analysis, the second and higher order FRFs contain additional information. These functions are directly related to the harmonics of the nonlinear FR, and can be estimated from them. E.g., the first, second and third harmonic and the DC component of the output can be expressed by (2), (3), (4) and (5), respectively:

$$\begin{aligned} y_I &= B_I\cos(\omega t + \varphi_I) \\ &= \{(A/2)G_1(\omega) + 3(A/2)^3 G_3(\omega,\omega,-\omega) + \cdots\}e^{j\omega t} \\ &\quad + \{(A/2)G_1(-\omega) + 3(A/2)^3 G_3(\omega,-\omega,-\omega) + \cdots\} \\ &\quad \times e^{-j\omega t} \end{aligned} \quad (2)$$

$$\begin{aligned} y_{II} &= B_{II}\cos(2\omega t + \varphi_{II}) \\ &= \{(A/2)^2 G_2(\omega,\omega) \\ &\quad + 4(A/2)^4 G_4(\omega,\omega,\omega,-\omega) + \cdots\}e^{2j\omega t} \\ &\quad + \{(A/2)^2 G_2(-\omega,-\omega) \\ &\quad + 4(A/2)^4 G_4(\omega,-\omega,-\omega,-\omega) + \cdots\}e^{-2j\omega t} \end{aligned} \quad (3)$$

$$\begin{aligned} y_{III} &= B_{III}\cos(3\omega t + \varphi_{III}) \\ &= \{(A/2)^3 G_3(\omega,\omega,\omega) \\ &\quad + 5(A/2)^5 G_5(\omega,\omega,\omega,\omega,-\omega) + \cdots\}e^{3j\omega t} \\ &\quad + \{(A/2)^3 G_3(-\omega,-\omega,-\omega) \\ &\quad + 5(A/2)^5 G_5(\omega,\omega,-\omega,-\omega,-\omega) + \cdots\}e^{-3j\omega t} \end{aligned} \quad (4)$$

$$y_{DC} = 2(A/2)^2 G_2(\omega,-\omega) + 6(A/2)^4 G_4(\omega,\omega,-\omega,-\omega) + \cdots \quad (5)$$

More details about the general nonlinear FR and Volterra series expansion can be found in Weiner and Spina (1980) or in some of our previous publications (Petkovska 2001; Petkovska 2005b; Petkovska and Do 1998).

A very important result of our analysis of adsorption kinetics by nonlinear FR is that the higher order functions defined on the particle level (correlating the changes of the adsorbate concentration in the particle and in the surrounding fluid, Petkovska 2001) have different shapes for different kinetic mechanisms. This fact can be used for reliable identification of the correct kinetic mechanism (Petkovska and Do 2000; Petkovska and Petkovska 2003; Petkovska 2005a). The higher order FRFs also enable estimation of additional system parameters.

Up to now, the NFR analysis has been applied to a number of, mostly isothermal, simple (Petkovska and Do 1998) and complex (Petkovska and Petkovska 2003; Petkovska 2005a) kinetic mechanisms, although some nonisothermal cases have also been analysed (Petkovska 2000). The analysis is mainly based on reservoir type adsorbers with periodic modulation of the reservoir volume or inlet flow rate (Petkovska and Do 1998; Petkovska 2001), which enable relatively easy extraction of the FRFs on the particle scale.

Nevertheless, the assumption of ideal mixing, which is typical for the reservoir type adsorbers, is not always met, especially for liquid-solid systems. For that reason, the NFR analysis was extended to chromatographic systems with periodic modulation of the inlet concentration. This analysis was successfully applied to estimation of equilibrium isotherms (Petkovska and Seidel-Morgenstern, 2005; Ilić et al., 2007a, 2007b, 2007c). On the other hand, estimation of the particle FRFs, which are needed for identification of the correct kinetic model, from the FRFs of a chromatographic column, is very difficult. As illustration, we give the mathematical expression of the first order FRF of a chromatographic column, derived for isothermal, plug-flow with axial dispersion case (Petkovska and Seidel-Morgenstern, 2005):

$$G_1(\omega) = \frac{2N(\lambda_2-\lambda_1)e^{\lambda_2}}{2N(\lambda_2 e^{\lambda_2-\lambda_1}-\lambda_1)+\lambda_1\lambda_2(1-e^{\lambda_2-\lambda_1})} \quad (6)$$

where N is the number of theoretical plates, and λ_1 and λ_2 are solutions of the corresponding characteristic equation:

$$\lambda_{1,2}(\omega) = N \pm \sqrt{N^2 + 2N\left(1 + F_1(\omega)\frac{1-\varepsilon}{\varepsilon}\frac{Q_s}{C_s}\right)j\omega} \quad (7)$$

In (7), $F_1(\omega)$ is the first order FRF on the particle scale, which contains the information about the adsorption kinetics (ε is the bed porosity and Q_s and C_s the steady-state concentrations in the stagnant and moving phases, respectively). Obviously, extracting the function $F_1(\omega)$ from $G_1(\omega)$ is

rather difficult. This difficulty increases considerably for the second, third and higher order FRFs.

This was our motivation for introducing the NFR-ZLC method. The idea is to use and combine the advantages of both methods:

- The potential to identify a model corresponding to the most probable kinetic mechanism and to estimate both the equilibrium and kinetic parameters of the identified model, which are characteristics of the NFR method and
- The potential to derive direct information about the processes on the particle level, by eliminating the influence of the adsorber, which is a characteristic of the ZLC method.

Fig. 1 Schematic picture of the NFR-ZLC system

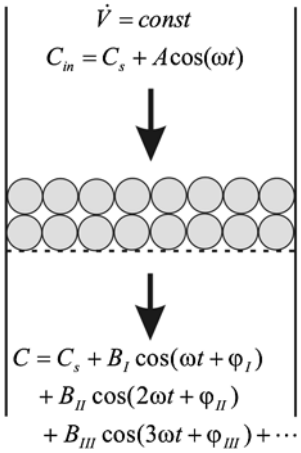

2 Definition and mathematical model of the NFR-ZLC system

The NFR-ZLC method is based on the ZLC apparatus in which the inlet concentration is modulated in a sinusoidal way around a chosen steady-state value. The system is shown schematically in Fig. 1. Owing to a very shallow adsorption bed used, the concentration of the effluent stream is considered equal to the concentration within the bed.

The mathematical model of the system shown in Fig. 1, for the case of isothermal conditions and constant flow rate, is given by the following material balance equation:

$$\gamma \frac{dc}{dt} + \beta \frac{d\langle q \rangle}{dt} = c_{in} - c \tag{8}$$

In (8) the concentrations in the fluid c, and in the particle q, as well as the inlet concentration c_{in}, are defined as nondimensional deviations from their steady-state values:

$$c = \frac{C - C_s}{C_s}, \qquad c_{in} = \frac{C_{in} - C_s}{C_s}, \qquad q = \frac{Q - Q_s}{Q_s} \tag{9}$$

and the parameters β and γ are defined as:

$$\gamma = \frac{\varepsilon V}{\dot{V}}, \qquad \beta = \frac{(1-\varepsilon) V Q_s}{\dot{V} C_s} \tag{10}$$

(V is the volume of the ZLC bed, ε its porosity and $\dot{V}$ the volumetric flow-rate). As the concentration in the particle is generally nonuniform, the average concentration $\langle q \rangle$ is used in (8).

The frequency response analysis assumes modulation of the input (in our case inlet concentration) around a previously established steady state value. Accordingly, the initial conditions for (8) are:

$$t < 0: \quad c = c_{in} = q = 0 \tag{11}$$

and the inlet concentration is:

$$t \geq 0: \quad c_{in} = A\cos(\omega t) \tag{12}$$

In order to get a complete mathematical model, an additional model equation, defining the mass transport on the particle level, is needed. The form of this equation depends on the kinetic mechanism. For the sake of generality, for the moment we will define the model on the particle scale by a general expression:

$$\langle q \rangle = \mathbf{F}(c) \tag{13}$$

In the frequency domain, the nonlinear operator $\mathbf{F}$ can be replaced by a sequence of frequency response functions of the first, second, third, ... order (Weiner and Spina 1980). The functions for different kinetic mechanisms, which can be found in our previous publications, have been reviewed in Petkovska (2005b).

3 Frequency response functions of the ZLC system

Let's denote the FRFs relating the outlet and the inlet concentrations (c and c_{in}) in the ZLC system with $G_1(\omega)$, $G_2(\omega_1, \omega_2)$, $G_3(\omega_1, \omega_2, \omega_3)$, etc.

For the cosinusoidal modulation of the inlet concentration:

$$c_{in} = A\cos(\omega t) = \frac{A}{2}(e^{j\omega t} + e^{-j\omega t}) \tag{12a}$$

using the Volterra series expansion, the outlet concentration can be represented in the following form:

$$\begin{aligned} c = {} & \frac{A}{2}(G_1(\omega)e^{j\omega t} + G_1(-\omega)e^{-j\omega t}) \\ & + \left(\frac{A}{2}\right)^2 (G_2(\omega,\omega)e^{2j\omega t} + 2G_2(\omega,-\omega)e^{0} \\ & + G_2(-\omega,-\omega)e^{-2j\omega t}) \\ & + \left(\frac{A}{2}\right)^3 (G_3(\omega,\omega,\omega)e^{3j\omega t} + 3G_3(\omega,\omega,-\omega)e^{j\omega t} \end{aligned}$$

$$+ 3G_3(\omega, -\omega, -\omega)e^{j\omega t} + G_3(-\omega, -\omega, -\omega)e^{-3j\omega t}) + \cdots \quad (14)$$

On the other hand, the concentrations in the particle and in the surrounding fluid ($\langle q\rangle$ and c) are also related by a set of FRFs, i.e. $F_1(\omega)$, $F_2(\omega_1, \omega_2)$, $F_3(\omega_1, \omega_2, \omega_3)$, etc. The concentration in the particle can, thus, be presented in the following way:

$$\begin{aligned}\langle q\rangle = {} & \frac{A}{2}(G_1(\omega)F_1(\omega)e^{j\omega t} + G_1(-\omega)F_1(-\omega)e^{-j\omega t}) \\ & + \left(\frac{A}{2}\right)^2 (G_2(\omega,\omega)F_1(2\omega)e^{2j\omega t} + 2G_2(\omega,-\omega) \\ & \times F_1(0)e^0 + G_2(-\omega,-\omega)F_1(-2\omega)e^{-2j\omega t}) \\ & + \left(\frac{A}{2}\right)^3 (G_3(\omega,\omega,\omega)F_1(3\omega)e^{3j\omega t} \\ & + 3G_3(\omega,\omega,-\omega)F_1(\omega)e^{j\omega t} \\ & + 3G_3(\omega,-\omega,-\omega)F_1(-\omega)e^{j\omega t} \\ & + G_3(-\omega,-\omega,-\omega)F_1(-3\omega)e^{-3j\omega t}) + \cdots \\ & + \left(\frac{A}{2}\right)^2 (G_1^2(\omega)F_2(\omega,\omega)e^{2j\omega t} \\ & + 2G_1(\omega)G_1(-\omega)F_2(\omega,\omega)e^0 \\ & + G_1^2(-\omega)F_2(-\omega,-\omega)e^{-2j\omega t}) \\ & + \left(\frac{A}{2}\right)^3 (2G_1(\omega)G_2(\omega,\omega)F_2(\omega,2\omega)e^{3j\omega t} \\ & + 2G_1(-\omega)G_2(-\omega,-\omega)F_2(-\omega,-2\omega)e^{-3j\omega t} + \cdots) \\ & + \left(\frac{A}{2}\right)^3 (G_1^3(\omega)F_3(\omega,\omega,\omega)e^{3j\omega t} \\ & + G_1^3(-\omega)F_3(-\omega,-\omega,-\omega)e^{-3j\omega t} + \\ & + 3G_1^2(\omega)G_1(-\omega)F_3(\omega,\omega,-\omega)e^{j\omega t} \\ & + 3G_1^2(-\omega)G_1(\omega)F_3(\omega,-\omega,-\omega)e^{-j\omega t}) + \cdots \end{aligned} \quad (15)$$

By substituting the expressions for c_{in}, c and $\langle q\rangle$ (defined by (12a), (14) and (15)) into (8), and applying the method of harmonic probing (collecting the terms with the same amplitude and frequency), a set of algebraic equations is obtained, defining the ZLC FRFs. Here are the expressions obtained for the first three FRFs, obtained by collecting the terms with $Ae^{j\omega t}$, $A^2e^{2j\omega t}$, A^2e^0 and $A^3e^{3j\omega t}$, respectively:

$$G_1(\omega) = \frac{1}{1 + \omega j(\gamma + \beta F_1(\omega))} \quad (16)$$

$$G_2(\omega,\omega) = -\frac{G_1^2(\omega)F_2(\omega,\omega)}{1 + 2\omega j(\gamma + \beta F_1(2\omega))}2\omega j\beta \quad (17)$$

$$G_2(\omega,-\omega) = 0 \quad (18)$$

$$\begin{aligned} & G_3(\omega,\omega,\omega) \\ & = -\frac{G_1^3(\omega)F_3(\omega,\omega,\omega) + G_1(\omega)G_2(\omega,\omega)F_2(\omega,2\omega)}{1 + 3\omega j(\gamma + \beta F_1(3\omega))} \\ & \quad \times 3\omega j\beta \end{aligned} \quad (19)$$

These expressions enable calculating of the FRFs of the ZLC system for any particular kinetic model. On the other hand, they also enable calculation of the FRFs defined on the particle level (the F-functions), from the FRFs on the ZLC level (the G-functions), which can be estimated directly from the FR experiments.

It is important to notice that the asymmetric second order function $G_2(\omega, -\omega)$ is zero for any kinetic mechanism. As a consequence, the function $F_2(\omega, -\omega)$, which was found very useful for mechanism identification (Petkovska and Do 2000; Petkovska and Petkovska 2003) can not be estimated from the NFR-ZLC experiments.

The analysis in this work will be limited to three common isothermal, rather simple kinetic models, corresponding to: film resistance control, micropore diffusion control and pore-surface diffusion control. The basic model equations for these mechanisms are listed below in the next section. The corresponding expressions for the first, second and third order FRFs are given in the Appendix, without any details about the derivation. The derivation procedure, together with a rather detailed derivation of the first and second order FRFs corresponding to these three mechanisms, can be found in Petkovska (2005b); Petkovska and Do (2000). The expressions for the third order FRFs are published here for the first time.

4 Kinetic models

4.1 Film resistance model

If the main resistance to the mass transfer can be lumped in the fluid film surrounding the particle, a film resistance model can be used:

$$\frac{dq}{dt} = k_m(c - \Gamma(q)) = k_m(c - \varphi^{-1}(q)) \quad (20)$$

where $k_m(1/s)$ is the mass transfer coefficient. The function φ, defining the adsorption isotherm, is generally nonlinear and its unique inverse Γ is assumed to exist. (This assumption is valid for all five isotherm types of the BDDT classification, Do 1998, but, for example, it is not valid for irreversible isotherm.)

In order to apply the nonlinear FR analysis, it is most convenient to express Γ in the Taylor series form:

$$\Gamma(q) = \tilde{a}_q q + \tilde{b}_q q^2 + \tilde{c}_q q^3 + \cdots \quad (21)$$

The FRFs corresponding to this mechanism, up to the third order, are given in the Appendix ((57) to (60)).

The time constant corresponding to this case, used in (57) to (60), is defined in the following way:

$$\tau_F = \frac{1}{\tilde{a}_q k_m} \tag{22}$$

4.2 Micropore diffusion model

If the dominant mass transfer resistance is in the microparticles, the adsorption process is controlled by the rate of micropore diffusion. For the one-dimensional case it can be described mathematically by the following equation:

$$\frac{\partial q}{\partial t} = \frac{1}{r_\mu^\sigma}\frac{\partial}{\partial r_\mu}\left(r_\mu^\sigma D_\mu \frac{\partial q}{\partial r_\mu}\right) \tag{23}$$

In this equation, q is the nondimensional concentration of the adsorbate in the micropores, at position r_μ, D_μ the micropore diffusion coefficient and σ the shape factor ($\sigma = 0$ for plane, $\sigma = 1$ for cylindrical and $\sigma = 2$ for spherical geometry). The boundary conditions for (23) are:

$$r_\mu = 0: \quad \frac{\partial q}{\partial r_\mu} = 0, \qquad r_\mu = R_\mu: \quad q = \varphi(c) \tag{24}$$

In (24) R_μ is the microparticle half-dimension and $\varphi(c)$ is again the adsorption equilibrium relation, which is generally nonlinear, and can be expanded into a Taylor series:

$$\varphi(c) = \tilde{a}_c c + \tilde{b}_c c^2 + \tilde{c}_c c^3 + \cdots \tag{25}$$

As q changes within the microparticle, the mean concentration has to be defined:

$$\langle q \rangle = \frac{\sigma + 1}{R_\mu^{\sigma+1}} \int_0^{R_\mu} r_\mu^\sigma q(r_\mu)\, dr_\mu \tag{26}$$

The corresponding FRFs up to the third order, derived for the case of constant diffusion coefficient and plane geometry ($\sigma = 0$) are given in the Appendix ((61) to (64)).

The time constant for this mechanism is defined as:

$$\tau_M = \frac{R_\mu^2}{D_\mu} \tag{27}$$

4.3 Pore-surface diffusion model

In a number of cases the adsorption kinetic is governed by particle diffusion which generally takes place by two parallel mechanisms: pore diffusion and surface diffusion. If the concentrations are again defined as nondimensional perturbations from their steady-state values, the one-dimensional pore-surface diffusion model can be described by the following equation:

$$(1-\varepsilon_p)\frac{\partial q_i}{\partial t} + \varepsilon_p'\frac{\partial c_i}{\partial t} = (1-\varepsilon_p)\frac{1}{r^\sigma}\frac{\partial}{\partial r}\left(D_s r^\sigma \frac{\partial q_i}{\partial r}\right) + \varepsilon_p'\frac{1}{r^\sigma}\frac{\partial}{\partial r}\left(D_p r^\sigma \frac{\partial c_i}{\partial r}\right) \tag{28}$$

where r is the particle space coordinate, c_i the concentration in the pores at position r, q_i the corresponding concentration of the adsorbed phase, D_s the surface diffusion coefficient and D_p the pore diffusion coefficient, ε_p is the particle porosity, and $\varepsilon_p' = \varepsilon_p C_{is}/Q_{is}$. Local equilibrium within the pores is commonly assumed:

$$\forall r: \quad q_i = \varphi(c_i) = \tilde{a}_c c_i + \tilde{b}_c c_i^2 + \tilde{c}_c c_i^3 + \cdots \tag{29}$$

The boundary conditions for (28) are:

$$r = 0: \quad \frac{\partial q_i}{\partial r} = \frac{\partial c_i}{\partial r} = 0, \qquad r = R: \quad c_i = c \tag{30}$$

(c is the concentration in the gas phase, as before, and R is the particle half-dimension).

The concentrations q_i and c_i are both functions of r. The mean concentration in the particle can be obtained as:

$$\langle q \rangle = \frac{\sigma + 1}{R^{\sigma+1}} \int_0^R r^\sigma \left(\frac{(1-\varepsilon_p)}{(1-\varepsilon_p)+\varepsilon_p'} q_i(r) + \frac{\varepsilon_p'}{(1-\varepsilon)+\varepsilon_p'} c_i(r)\right) dr \tag{31}$$

The corresponding FRFs up to the third order, derived for constant diffusion coefficients and plane geometry ($\sigma = 0$) are listed in the Appendix ((66) to (69)).

The time constant for the pore-surface diffusion mechanism can be defined as:

$$\tau_{PS} = \frac{R^2}{D_{eff}} \tag{32}$$

where D_{eff} is the effective, or apparent, diffusivity:

$$D_{eff} = \frac{(1-\varepsilon_p)D_s a_p + \varepsilon_p' D_p}{(1-\varepsilon_p)a_p + \varepsilon_p'} = \frac{(1-\varepsilon_p)D_s a_p Q_{is} + \varepsilon_p D_p C_{is}}{(1-\varepsilon_p)a_p Q_{is} + \varepsilon_p C_{is}} \tag{33}$$

5 Simulation of ZLC FRFs

In this section, we show some simulation results of the ZLC FRFs, obtained for the three kinetic mechanisms defined in the previous section. The model parameters used for these

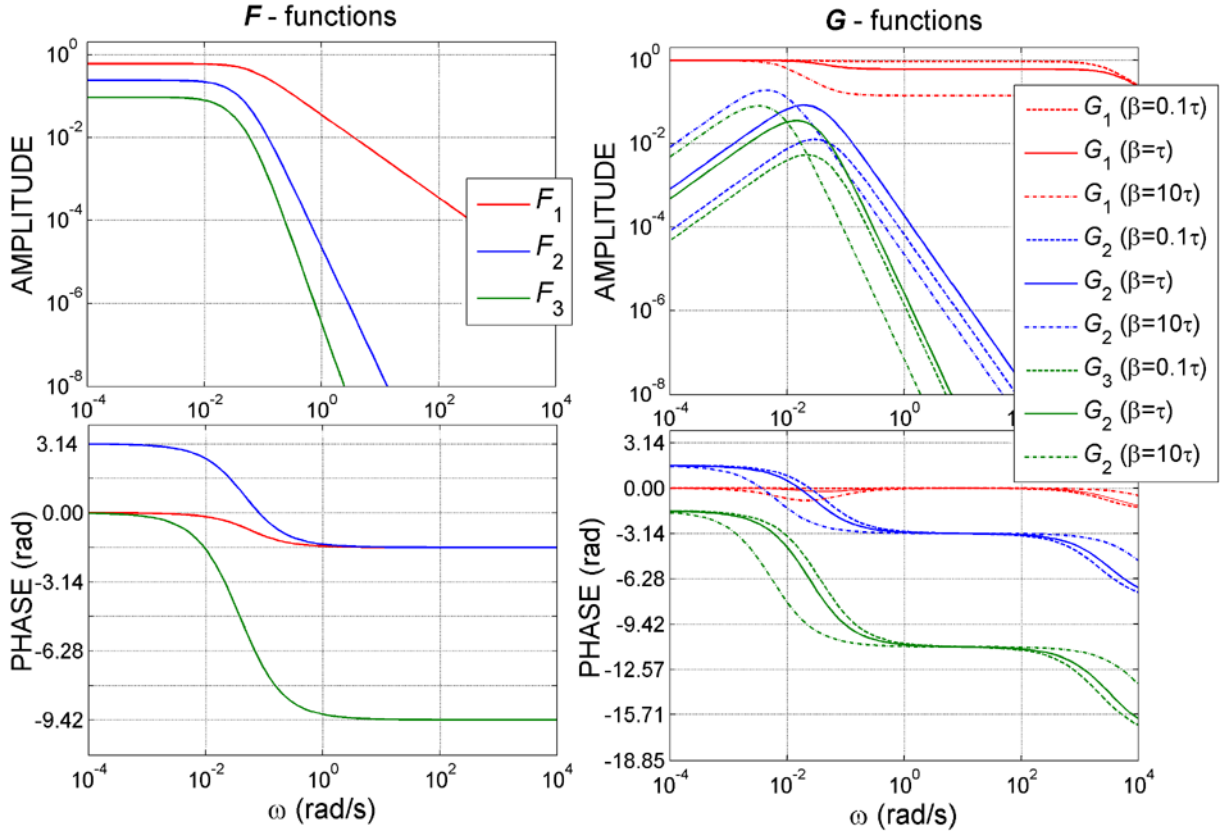

Fig. 2 Particle (F) and ZLC (G) FRFs for film-resistance control

Table 1 Model parameters used for simulation

Film-resistance model

$\tilde{a}_q = 1.64$, $\tilde{b}_q = 1.05$, $\tilde{c}_q = 0.672$, $k_m = 0.0355$ 1/s ($\tau_F = 17.17$ s)

Micropore diffusion model

$\tilde{a}_c = 0.610$, $\tilde{b}_c = -0.238$, $\tilde{c}_c = 0.093$, $R_\mu = 1 \times 10^{-5}$ m,
$D_\mu = 5.82 \times 10^{-12}$ m^2/s ($\tau_M = 17.17$ s)

Pore-surface diffusion model

$\tilde{a}_c = 0.610$, $\tilde{b}_c = -0.238$, $\tilde{c}_c = 0.093$, $R = 1 \times 10^{-4}$ m,
$D_{eff} = 5.82 \times 10^{-10}$ m^2/s, $D_s = 2 \times 10^{-10}$ m^2/s, $\varepsilon_p = 0.2$,
$\varepsilon'_p = 4.66 \times 10^{-5}$ ($\tau_{PS} = 17.17$ s)

Common parameters

$\beta = 0.1\tau, \tau, 10\tau$, $\gamma = 0.0004$ s

simulations are listed in Table 1. These values roughly correspond to the system analyzed in Brandani (1998).

The parameters for all three mechanisms correspond to the same adsorption isotherm and to the identical time constants on the particle level. On the ZLC level, two other time constants can be defined: β and γ. They correspond to the rates of accumulation in the particles and in the interstitial fluid in the bed, respectively. Owing to practically negligible accumulation in the interstitial fluid, the time constant γ has a very small value and practically doesn't influence the overall dynamics of the system. Generally, the dynamics of the ZLC system is governed by two time constants, τ and β.

The simulation results, corresponding to the film-resistance, micropore and pore-surface diffusion models, are shown in Figs. 2, 3 and 4, respectively. In these figures, the FRFs on both particle (the F-functions) and ZLC level (the G-functions) are presented, in the form of standard Bode plots (amplitudes vs. frequency in log-log, and phases vs. frequency in semi-log diagrams). In order to investigate the interplay between the time constants τ and β, the ZLC FRFs were simulated for 3 values of β: $\beta = 0.1\tau$, $\beta = \tau$ and $\beta = 10\tau$.

The right-hand parts of Figs. 3, 4 and 5 show that the shapes of the G-functions depend, not only on the kinetic mechanism, but also on the value of the time constant β. For this reason, the G-functions are not very convenient for identification of the kinetic model. Also, it can be seen that the amplitudes of the second and third order functions generally decrease when the ratio of the column and particle time constants β/τ increases. One should also notice that the maximums of the amplitudes of $G_2(\omega, \omega)$ and $G_3(\omega, \omega, \omega)$ move into the range of higher frequencies when β/τ increases.

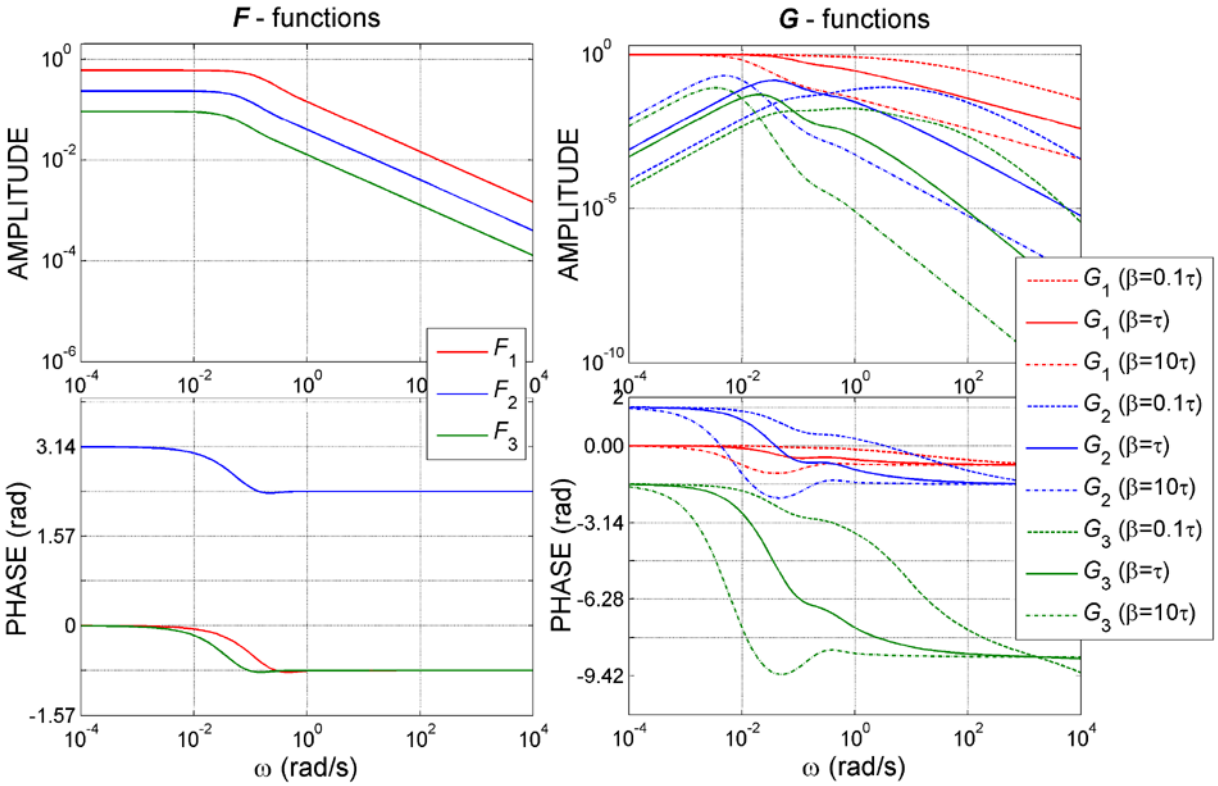

Fig. 3 Particle (F) and ZLC (G) FRFs for micropore diffusion control

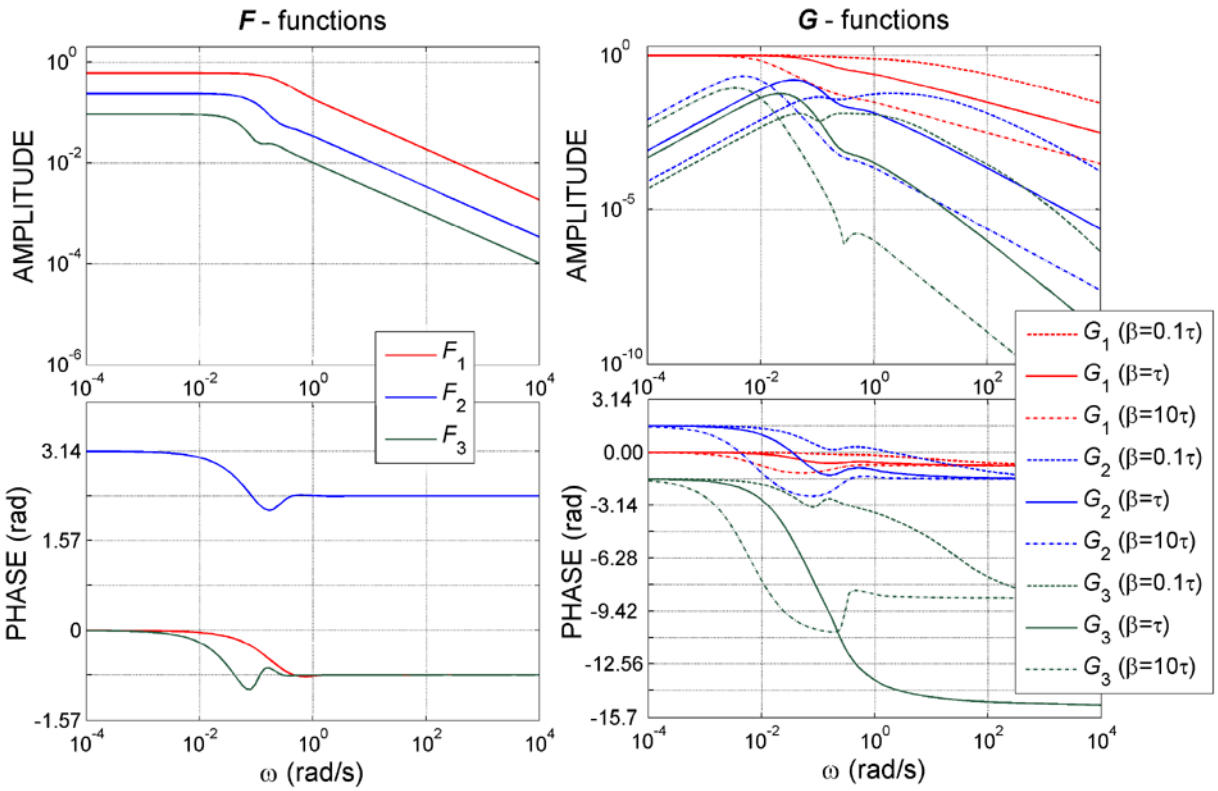

Fig. 4 Particle (F) and ZLC (G) FRFs for pore-surface diffusion control

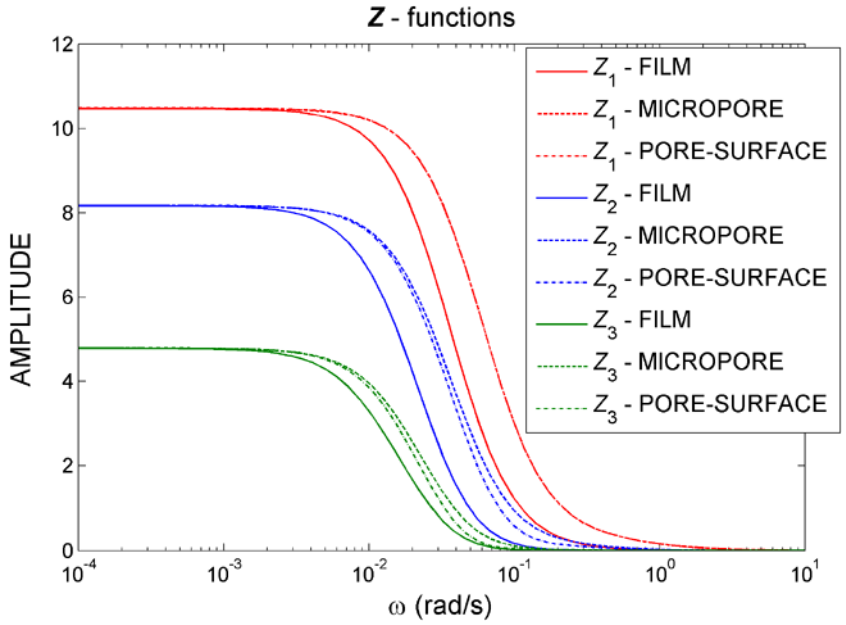

Fig. 5 The Z-functions for the three mechanisms

6 Model identification and parameters estimation

6.1 Model identification

As mentioned in the previous section, the shapes of the G-functions, defining the FRFs on the ZLC level, change somewhat with the change of the time constant β, so they are not very convenient for identification of the underlying kinetic model. Nevertheless, the inspection of the F-functions in Figs. 2, 3 and 4 shows the following:

(1) All three FRFs corresponding to the film-resistance model have different high-frequency asymptotes than the corresponding FRFs for the diffusion mechanisms. Consequently, the discrimination between the film-resistance and the diffusion models is possible even from the characteristics of the first order FRF $F_1(\omega)$.
(2) The high-frequency asymptotes for all three FRFs corresponding to micropore and pore-surface diffusion models have similar features. Nevertheless, the shapes of the second and third function, $F_2(\omega,\omega)$ and $F_3(\omega,\omega,\omega)$, for the two mechanisms, are different.

A detailed discussion on the differences in the patterns of the FRFs corresponding to the three models analysed in this manuscript can be found in Petkovska and Do (2000).

The important result is that the FRFs on the particle level (the F-functions) have unique patterns for all three mechanisms, and can, therefore, be used for model identification.

The F-functions can be easily calculated from (16), (17) and (19), once the G-functions are estimated from experimental FR results.

6.2 Estimation of equilibrium parameters

The equilibrium behaviour can easily be extracted from the low-frequency asymptotes of the particle FRFs, in the following way: the first, second, third, etc., derivatives of the adsorption isotherm can be obtained directly from the low-frequency asymptotes of the first, second, third, etc. particle FRFs. Using the expressions for the particle FRFs from the Appendix, the following results were obtained:

(a) *For the film resistance model*

$$\lim_{\omega\to 0} F_1(\omega) = \frac{1}{\tilde{a}_q} = \tilde{a}_c = \left.\frac{\partial Q}{\partial C}\right|_s \frac{C_s}{Q_s} \tag{34}$$

$$\lim_{\omega\to 0} F_2(\omega,\omega) = -\frac{\tilde{b}_q}{\tilde{a}_q^3} = \tilde{b}_c = \frac{1}{2}\left.\frac{\partial^2 Q}{\partial C^2}\right|_s \frac{C_s^2}{Q_s} \tag{35}$$

$$\lim_{\omega\to 0} F_3(\omega,\omega,\omega) = \frac{2\tilde{b}_q^2}{\tilde{a}_q^5} - \frac{\tilde{c}_q}{\tilde{a}_q^4} = \tilde{c}_c = \frac{1}{6}\left.\frac{\partial^3 Q}{\partial C^3}\right|_s \frac{C_s^3}{Q_s} \tag{36}$$

The fact that $\tilde{a}_q$, $\tilde{b}_q$ and $\tilde{c}_q$ on one, and $\tilde{a}_c$, $\tilde{b}_c$ and $\tilde{c}_c$, on the other hand, correspond to inverse functions Γ and φ, is used in these equations.

(b) *For the micropore diffusion model*

$$\lim_{\omega\to 0} F_1(\omega) = \tilde{a}_c \tag{37}$$

$$\lim_{\omega\to 0} F_2(\omega,\omega) = \tilde{b}_c \tag{38}$$

$$\lim_{\omega\to 0} F_3(\omega,\omega,\omega) = \tilde{c}_c \tag{39}$$

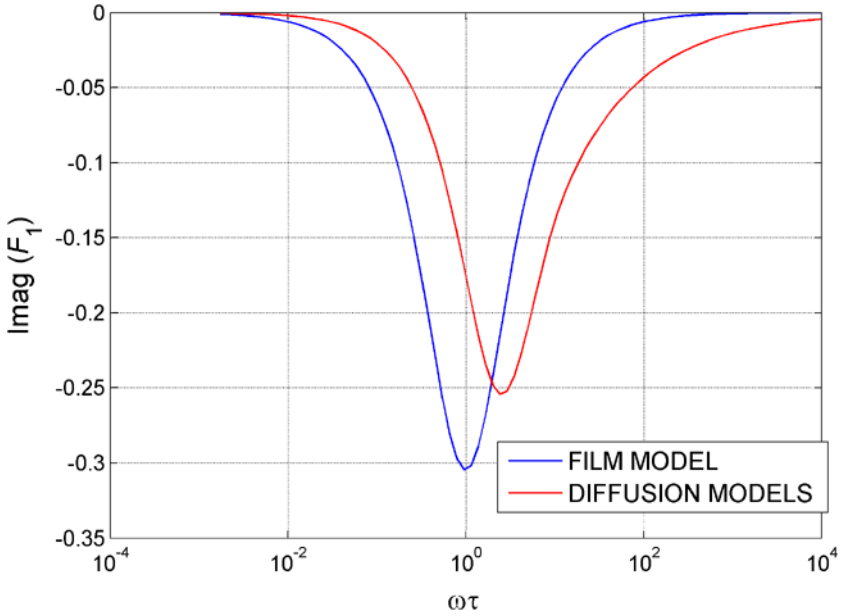

Fig. 6 Imaginary part of the first order particle FRF for the film-resistance and diffusion models—estimation of the process time constants

(c) *For the pore-surface diffusion model*

$$\lim_{\omega\to 0} F_1(\omega) = \frac{\varepsilon_p' + (1-\varepsilon_p)\tilde{a}_c}{\varepsilon_p' + 1 - \varepsilon_p} = \frac{\varepsilon_p C_{is} + (1-\varepsilon_p)\tilde{a}_c Q_{is}}{\varepsilon_p C_{is} + (1-\varepsilon_p) Q_{is}} \tag{40}$$

$$\lim_{\omega\to 0} F_2(\omega,\omega) = \frac{(1-\varepsilon_p)\tilde{b}_c}{\varepsilon_p' + 1 - \varepsilon_p} = \frac{(1-\varepsilon_p)\tilde{b}_c Q_{is}}{\varepsilon_p C_{is} + (1-\varepsilon_p) Q_{is}} \tag{41}$$

$$\lim_{\omega\to 0} F_2(\omega,\omega,\omega) = \frac{(1-\varepsilon_p)\tilde{c}_c}{\varepsilon_p' + 1 - \varepsilon_p} = \frac{(1-\varepsilon_p)\tilde{c}_c Q_{is}}{\varepsilon_p C_{is} + (1-\varepsilon_p) Q_{is}} \tag{42}$$

Nevertheless, the equilibrium data can also be estimated directly from the ZLC FRFs, without estimating the FRFs on the particle level. If the following functions are defined:

$$Z_1(\omega) = -\frac{\mathrm{Im}(G_1(\omega))}{\omega} \tag{43}$$

$$Z_2(\omega,\omega) = \frac{G_2(\omega,\omega)}{\omega} \tag{44}$$

$$Z_3(\omega,\omega,\omega) = \frac{G_3(\omega,\omega,\omega)}{\omega} \tag{45}$$

it can easily be shown that:

$$\lim_{\omega\to 0} Z_1(\omega) = \lim_{\omega\to 0} \beta F_1(\omega) \tag{46}$$

$$\lim_{\omega\to 0} Z_2(\omega,\omega) = \lim_{\omega\to 0} 2\beta F_2(\omega,\omega) \tag{47}$$

$$\lim_{\omega\to 0} Z_3(\omega,\omega,\omega) = \lim_{\omega\to 0} 3\beta F_3(\omega,\omega,\omega) \tag{48}$$

The Z-functions corresponding to the G-functions for the case $\beta = \tau$ in Figs. 2, 3, and 4, are shown in Fig. 5.

Once the isotherm derivatives have been estimated, they can be used for derivation of the appropriate isotherm relation. If the type of the isotherm is already known or suspected, its parameters can be obtained by fitting the analytical expressions for the first, second and third derivatives to the experimentally estimated values. It was shown that reliable isotherms can be obtained in this way from FR experiments performed at only two or three steady-state concentrations (Ilić et al. 2007c).

On the other hand, if the isotherm type is completely unknown, the isotherm derivatives determined from the FR experiments at several steady-state concentrations can be used to generate additional isotherm points, by using Taylor series expansion, as explained in Petkovska and Seidel-Morgenstern (2005).

6.3 Estimation of the kinetic parameters

The problem of estimation of the kinetic parameters from linear FR characteristic functions, for simple isothermal kinetic models, has been solved long ago (Yasuda 1982). The process time constant can be estimated from the extremum of the so-called "out-of-phase" function (Yasuda 1982), which is identical to the negative imaginary part of the first order particle FRF $F_1(\omega)$ (Park et al. 1998). The imaginary parts of the $F_1(\omega)$ functions, corresponding to the film resistance mechanism and a single diffusion mechanism and plane geometry are shown in Fig. 6 (the forms of the functions $F_1(\omega)$ for the micropore and pore-surface diffusion

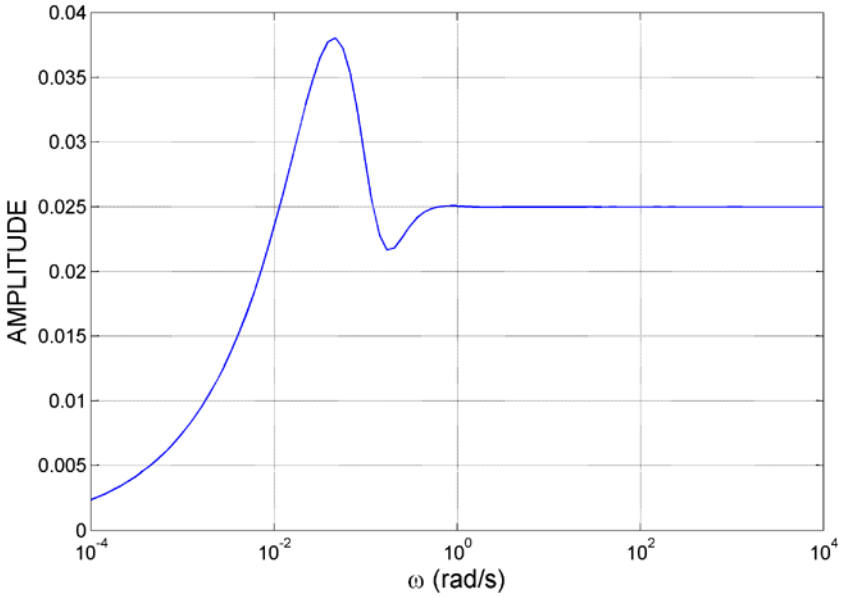

Fig. 7 The function $W(\omega)$—estimation of the surface diffusion coefficient (pore-surface diffusion mechanism)

mechanisms are identical). The minimums of these curves correspond to: $\omega\tau = 1$ for the film-resistance model and $\omega\tau = 2.5492$ for the diffusion models and plane geometry. Once the process time constant is known, it is easy to calculate the corresponding kinetic parameter (k_m for the film resistance, D_μ for the micropore or D_{eff} for the pore-surface mechanism), using the time constant definitions ((22), (27) or (32), respectively).

In addition to this, the nonlinear FR method also enables estimation of separate values of the pore and surface diffusion coefficients for the case of pore-surface diffusion mechanism. If the following function, based on the second order FRF, is defined:

$$W(\omega) = F_2(\omega, \omega)\sqrt{\omega} \tag{49}$$

it can be shown that it has a high-frequency asymptote:

$$\lim_{\omega\to\infty} W(\omega) = \frac{(1-\varepsilon_p)\tilde{b}_c}{1-\varepsilon_p+\varepsilon'_p} 0.207(1-j)\frac{D_{eff}+\sqrt{2}D_s}{R\sqrt{D_{eff}}} \tag{50}$$

which enables estimation of the surface diffusion coefficient, assuming the equilibrium parameters and the effective diffusion coefficient D_{eff} have been estimated previously. Knowing D_s and D_{eff} enables calculation of the pore diffusion coefficient D_p as well. The graphic representation of the function $W(\omega)$ is shown in Fig. 7.

7 Numerical experiments

In order to illustrate the proposed NFR-ZLC method and its procedure, some numerical experiments were performed. The numerical results were used as "quasi experimental" data. In principle, the procedure does not depend on the particular kinetic mechanism. For that reason, the numerical experiments were performed for only one mechanism. The film resistance control model was chosen as the simplest one from the point of view of the numerical solution of the model equation.

The frequency responses were simulated by numerical integration of the model equation (20). The simulations were performed with the same model parameters as used in Sect. 4, for $\beta = \tau$, for three input amplitudes ($A = 0.1$, 0.5 and 0.9, corresponding to 10%, 50% and 90% of the steady-state concentration) and for a number of frequencies. Numerical experiments in which random noise with 0.5% amplitude (relative to the steady-state concentration) was added to the simulated concentrations, were also performed. Although 0.5% noise amplitude might seem small, it is actually overestimated, keeping in mind that in the linear FR method the amplitudes of the input modulations are kept in the range from 1% (Song and Rees 1996) to 5% (Wang et al. 2003; Wang and LeVan 2007).

These simulated results were used as "quasi-experimental" data and the FRFs on the column and particle level were estimated from them and used for estimation of the equilibrium and kinetic parameters. This estimation is performed in four steps:

Step 1. Estimation of different harmonics of the output. This step is performed by applying the fast Fourier transform to the simulated "quasi-experimental" data, and calculating the amplitudes and phases of different harmonics from the transform. As illustration, in Fig. 8 we show the amplitudes of different harmonics, obtained for $\omega = 0.01$ rad/s and three input amplitudes. As the amplitudes of the

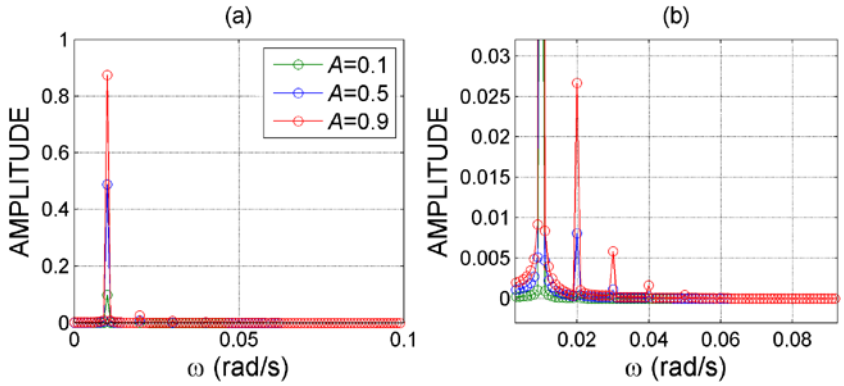

Fig. 8 Results of Fourier analysis of the ZLC output for $\omega = 0.01$ rad/s and $A = 0.1, 0.5$ and 0.9

second and higher harmonics are much smaller than those of the first (basic) one, in Fig. 8b we give an enlarged picture of the second and higher harmonics. Figure 8 shows that the amplitudes of the second and higher harmonics increase considerably with the increase of the input amplitude A. Actually, for $A = 0.1$, only the first and second harmonic can be detected, while for $A = 0.5$ and $A = 0.9$, one can detect up to the fourth and fifth harmonic, respectively.

Step 2. Estimation of the ZLC FRFs (the G-functions). As mentioned in the introduction, the FRFs of a nonlinear system are directly related to the harmonics of the nonlinear FR. These relations, for the first three harmonics, are defined by (2), (3) and (4). In the complex domain, these equations become:

$$Y_I = G_1(\omega)X + \frac{3}{4}G_3(\omega,\omega,-\omega)X^2\bar{X} + \cdots \tag{51}$$

$$Y_{II} = \frac{1}{2}G_2(\omega,\omega)X^2 + \frac{1}{2}G_4(\omega,\omega,\omega,-\omega)X^3\bar{X} + \cdots \tag{52}$$

$$Y_{III} = \frac{1}{4}G_3(\omega,\omega,\omega)X^3 + \frac{5}{16}G_5(\omega,\omega,\omega,\omega,-\omega)X^4\bar{X} + \cdots \tag{53}$$

where, Y_I, Y_{II} and Y_{III} are the Fourier transforms of the first, second and third harmonic, respectively, X is the Fourier transform of the input, and $\bar{X}$ its complex-conjugate.

Nevertheless, if the higher harmonics are negligible, these equations can be simplified, by keeping only the dominant terms containing $G_1(\omega)$, $G_2(\omega,\omega)$ and $G_3(\omega,\omega,\omega)$, respectively:

$$Y_I \approx G_1(\omega)X \tag{54}$$

$$Y_{II} \approx \frac{1}{2}G_2(\omega,\omega)X^2 \tag{55}$$

$$Y_{III} \approx \frac{1}{4}G_3(\omega,\omega,\omega)X^3 \tag{56}$$

In our analysis, we use these simplified equations.

Step 3. Calculation of the particle FRFs (the F-functions). The particle FRFs are calculated from the ZLC FRFs estimated in the previous step. The expressions for calculating the F-functions can be derived directly from (16), (17) and (19).

In Fig. 9, we show the G- and F-functions estimated from the numerically generated data, with input amplitudes $A = 0.1, 0.5$ and 0.9. It can be seen that the FRFs estimated from the numerical solution agree very well with the theoretical functions. In the low-frequency range, the agreement was slightly worse for higher input amplitudes. This is not unexpected, as the validity of (68) to (70) decreases with the increase of A. On the other hand, it can also be seen that the third order functions can not be estimated from the experiments with $A = 0.1$. This is in accordance with the results shown in Fig. 8, that the third harmonic of the output for $A = 0.1$ is negligible and can not be detected. Also, the second and third order FRFs can not be estimated for higher frequencies. The limiting frequencies for which these FRFs can be estimated increase with the increase of the input amplitude. Generally, we could say that smaller input amplitudes should be used for the experiments at lower frequencies and in the middle-frequency range, while larger input amplitudes should be used for higher frequencies.

The G- and F-functions estimated from the numerical data to which noise has been added are presented in Fig. 10. It can be seen that the estimated first order FRFs are practically unaffected by the noise, while the second and third order FRFs are more influenced. This influence is more pronounced for lower input amplitudes and for higher frequencies.

Step 4. Estimation of the equilibrium and kinetic data. Finally, in Fig. 11 we show the Z-functions (defined by (43)–(45)) and in Fig. 12 the imaginary part of $F_1(\omega)$, estimated from the numerically simulated data. As explained in Sects. 6.2 and 6.3, these figures can be used for estimation of the equilibrium and kinetic parameters of the underlying model.

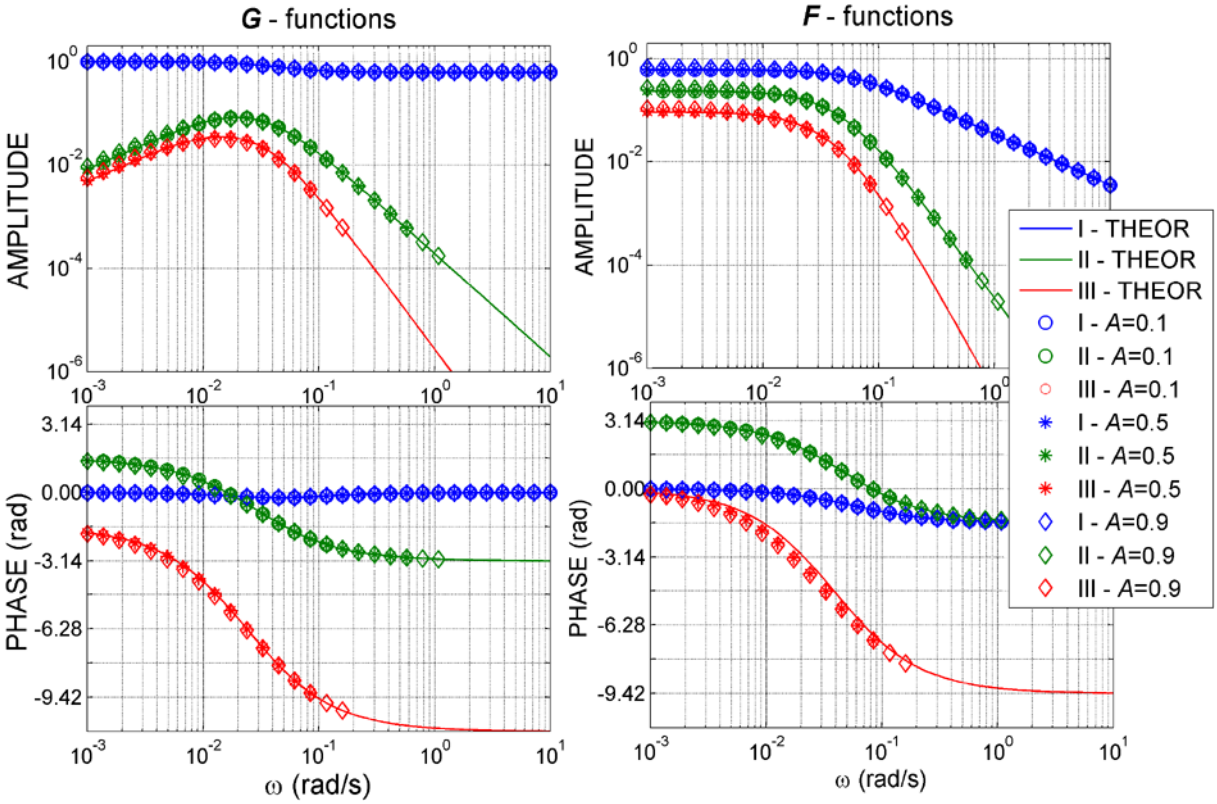

Fig. 9 Estimated G- and F-functions from the numerically simulated ZLC output concentrations

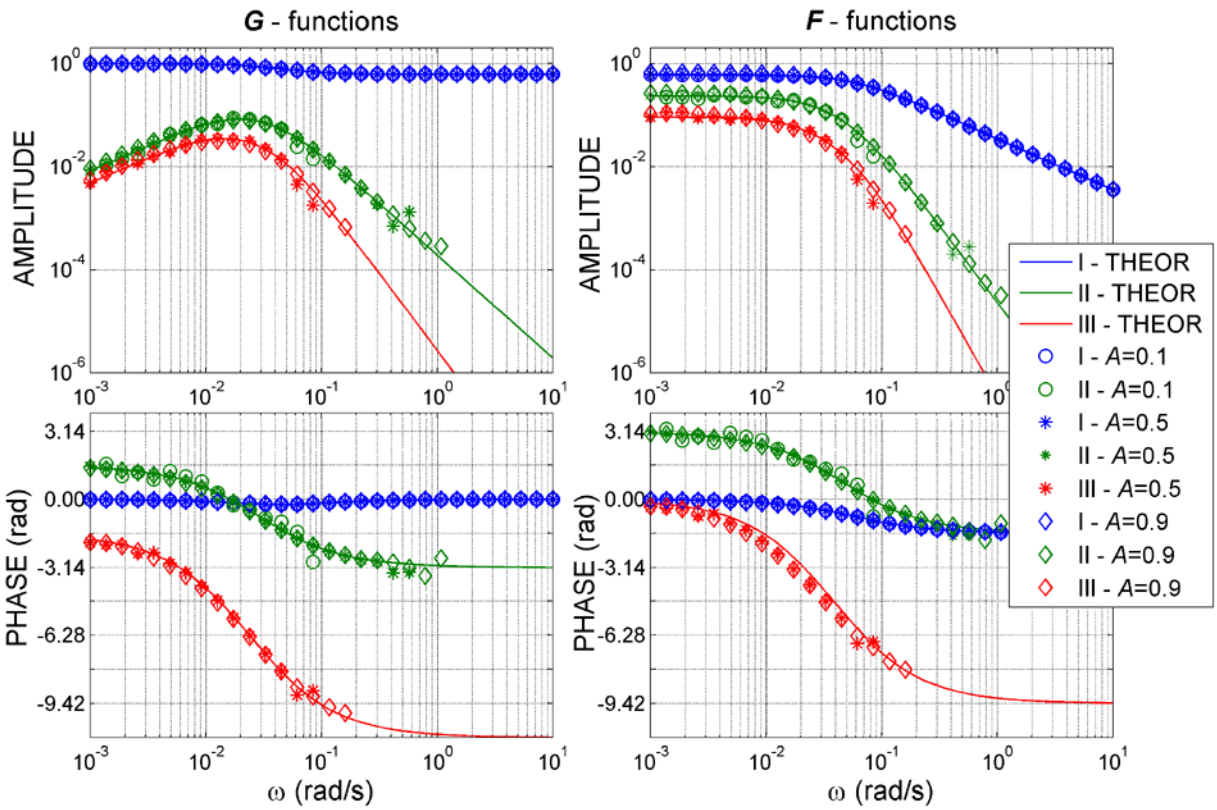

Fig. 10 Estimated G- and F-functions from the numerically simulated ZLC output concentrations with added noise

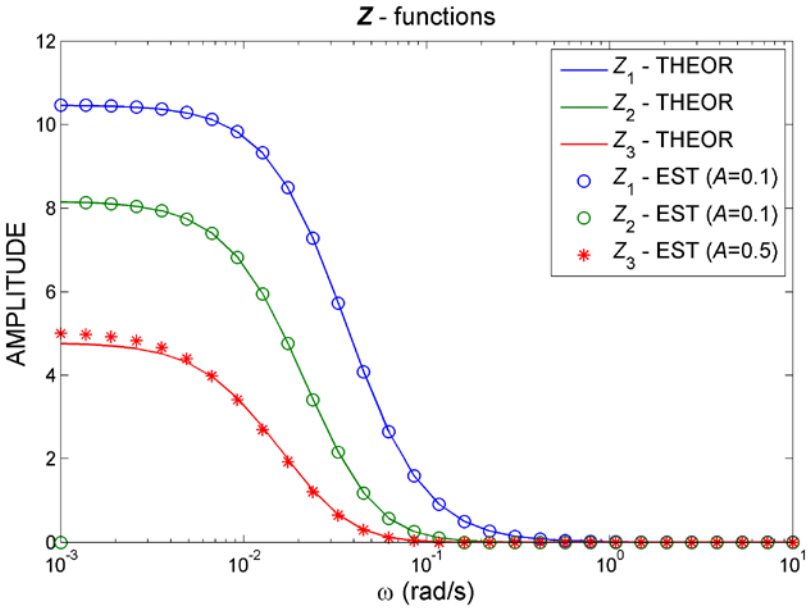

Fig. 11 The Z-functions estimated from the numerically simulated outlet concentrations

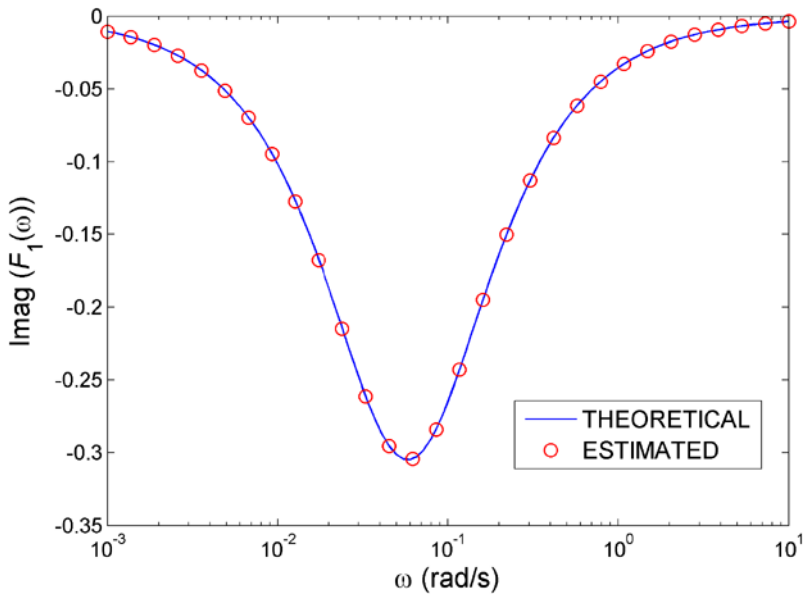

Fig. 12 The imaginary part of the first order particle FRF, estimated from numerically simulated concentrations

The following values were obtained from our numerically generated data:

$$\tilde{a}_c = \lim_{\omega\to 0} Z_1(\omega)/\beta = 0.61 \;\Rightarrow\; \tilde{a}_q = 1.64$$

$$\tilde{b}_c = \lim_{\omega\to 0} Z_2(\omega)/2/\beta = -0.237 \;\Rightarrow\; \tilde{b}_q = 1.044$$

$$\tilde{c}_c = \lim_{\omega\to 0} Z_3(\omega)/3/\beta = 0.097 \;\Rightarrow\; \tilde{c}_q = 0.630$$

$$\omega_{\min} = 0.062 \text{ rad/s} \;\Rightarrow\; \tau_{\mathrm{M}} = 16.1 \text{ s} \;\Rightarrow\; k_m = 0.038 \text{ 1/s}$$

By comparison with the model parameters listed in Table 1, it can be seen that the estimated values are very close to the original values used for simulation.

The first three steps of the presented procedure are identical for any kinetic mechanism of adsorption. In principle, the last step, estimation of the model parameters can be slightly different, depending on the identified model. If we limit our discussion to the three kinetic mechanisms considered in this manuscript, estimation of the model parameters for the micropore diffusion mechanism would be practically identical, and for the pore-surface diffusion mechanism similar as for the film resistance mechanism: the isotherm derivatives can be estimated from the low-frequency asymptotes of the F- or Z-functions, and the time constant (implying the information about the micropore or effective diffusion coefficient) from the minimum of imag$(F_1(\omega))$. For the case of pore-surface diffusion mechanism, the "experimen-

tal" function $W(\omega)$ (defined by (50)) is also needed, in order to estimate the separate values of the surface and pore diffusion coefficients. Regarding the fact that these values are estimated from the horizontal high-frequency asymptote of the W-function, these values can be estimated correctly only if this asymptotic region is reached. For the simulated example presented in Sect. 6, the asymptotic behaviour is achieved for $\omega \approx 1$ rad/s (see Fig. 7).

Naturally, the model parameters can be estimated more precisely by fitting the complete experimental F-functions, using a nonlinear least square procedure. Nevertheless, fast and easy estimation of their approximate values from the asymptotes and extrema of the F-functions is very significant, as it provides very good first guesses for the least-square optimisation.

8 Discussion on some practical aspects of the NFR-ZLC method

The NFR-ZLC method is a completely new method, introduced in this paper. Accordingly, there are no experimental data in the literature which could be used for analysis and discussion. Nevertheless, there are certain aspects regarding the practical application of the method that can be foreseen.

(1) In principle, the method can be performed using the standard ZLC apparatus, but with modulation of the input concentration in a sinusoidal way. Such modulation is possible experimentally and has already been reported (Ilić et al. 2007c; Wang and LeVan 2007).

(2) Like in the classical linear FR method, one of the limitations of the method lies in the fact that the input modulation is produced by mechanical means and that, consequently, the highest frequencies that can be physically attained are rather limited (the orders of magnitude reported in the literature are 1 to 10 Hz (Wang and LeVan 2007; Song and Rees 1996)). This limitation is very important for the NFR-ZLC method, as the high frequency behaviour of the second and third order FRFs are used for model discrimination. The influence of the β/τ ratio, analysed in Sect. 5 can also be re-evaluated from this aspect, as the increase of this ratio moves the maximums of the second and third order FRFs into the higher frequency range. The results presented in Sect. 5 show that it is recommendable that this ratio is $\sim$1, or smaller. The time constant on the column scale, β, can be adjusted to some extent, by changing the volumetric flow-rate. For that reason, having a rough estimate of the time constant on the particle scale, τ, would be very useful, so some preliminary step response experiments are recommended.

(3) The correct choice of the amplitudes of the input concentration modulation is also very important for proper application of the NFR-ZLC method. In principle, the amplitudes should be large enough that the first three harmonics of the output can be estimated, but, on the other hand small enough that higher harmonics are not significant. The optimal amplitude values depend on the system nonlinearity and vary from one system to another. Also, as shown in Sect. 6, the optimal input amplitudes are different for experiments at different frequencies. For that reason, some preliminary experiments are recommended.

(4) The analysis of the NFR-ZLC method presented here was performed for isothermal cases. Nevertheless, if the heat effects are not negligible, the method can be extended by defining additional sets of FRFs and taking into account both concentration and temperature changes (in a similar way as in Petkovska 2001). Appropriate temperature measurements would be important for proper application of the method to nonisothermal cases.

9 Conclusions

The theoretical analysis presented in this manuscript shows that the newly introduced, NFR-ZLC technique, which is based on nonlinear frequency response of a "zero length" column and the corresponding higher order FRFs, is feasible and shows good potential for identification of the kinetic model and estimation of both equilibrium and kinetic parameters of adsorption systems. The FRFs of the ZLC system are determined by the type of the kinetic mechanism and the corresponding kinetic parameters, but also by the dominant time constant on the column level. The numerical simulations show that it is recommendable that the time constant on the column level is of the same order of magnitude as the time constant on the particle level, or larger, in order to improve the chances for estimation of the higher order FRFs from the ZLC FR measurements.

The complete procedure of the NFR-ZLC method, leading to identification of the kinetic mechanism and estimation of the equilibrium and kinetic parameters is given. An illustration of this procedure, based on numerically generated data for the simple case of film-resistance control, proves that the procedure is rather simple and straightforward.

In this work, the analysis of the applicability of the NFR-ZLC method was limited only to three simple kinetic mechanisms (film-resistance, micropore diffusion and pore-surface diffusion). For these three mechanisms it was clearly shown how the method can lead to identification of the correct kinetic mechanism and to estimation of the local derivatives of the adsorption isotherm and the values of the main kinetic parameters. The analysis can easily be extended to other kinetic mechanisms.

Acknowledgements This work was supported by the Serbian Ministry of Science in the frame of Project No. 142014G.

Appendix: The particle FRFs up to the third order

The first and second order FRFs have already been presented in Petkovska and Do (2000), together with some details about their derivation. The expressions given here are presented in a slightly different form, which is more comprehensive. The third order FRFs are published here for the first time.

(1) Film resistance model

$$F_1(\omega) = \frac{1/\tilde{a}_q}{\tau_F \omega j + 1} \tag{57}$$

$$F_2(\omega,\omega) = -\frac{\tilde{b}_q}{\tilde{a}_q^3}\left(\frac{1}{2\tau_F\omega j+1}\right)\left(\frac{1}{\tau_F\omega j+1}\right)^2 \tag{58}$$

$$F_2(\omega,-\omega) = -\frac{\tilde{b}_q}{\tilde{a}_q^3}\frac{1}{1+\tau_F^2\omega^2} \tag{59}$$

$$F_3(\omega,\omega,\omega) = -\frac{2\tilde{b}_q F_1(\omega)F_2(\omega,\omega)+\tilde{c}_q F_1^3(\omega)}{\tilde{a}_q(1+3\tau_F\omega j)} \tag{60}$$

(2) Micropore diffusion model

The expressions listed here correspond to constant micropore diffusion coefficient and planar geometry.

$$F_1(\omega) = \tilde{a}_c\frac{\tanh(\omega_M^*)}{\omega_M^*} \tag{61}$$

$$F_2(\omega,\omega) = \tilde{b}_c\frac{\tanh(\sqrt{2}\omega_M^*)}{\sqrt{2}\omega_M^*} \tag{62}$$

$$F_2(\omega,\omega) = \tilde{b}_c \tag{63}$$

$$F_3(\omega,\omega,\omega) = \tilde{c}_c\frac{\tanh(\sqrt{3}\omega_M^*)}{\sqrt{3}\omega_M^*} \tag{64}$$

where:

$$\omega_M^* = \sqrt{j\tau_M\omega} \tag{65}$$

(3) Pore-surface diffusion model

The expressions given here correspond to constant pore and surface diffusion coefficients and planar geometry.

$$F_1(\omega) = \frac{(1-\varepsilon_p)\tilde{a}_c+\varepsilon_p'}{(1-\varepsilon_p)+\varepsilon_p'}\frac{\tanh(\omega_{PS}^*)}{\omega_{PS}^*} \tag{66}$$

$$F_2(\omega,\omega) = \frac{(1-\varepsilon_p)\tilde{b}_c}{1-\varepsilon_p+\varepsilon_p'}\left[\left(1-\frac{D_s}{D_{eff}}\right)\frac{\tanh(\omega_{PS}^*)}{\omega_{PS}^*}+\left(\frac{D_s}{D_{eff}}-\left(1-\frac{D_s}{D_{eff}}\right)\tanh^2(\omega_{PS}^*)\right)\frac{\tanh(\sqrt{2}\omega_{PS}^*)}{\sqrt{2}\omega_{PS}^*}\right] \tag{67}$$

$$F_2(\omega,-\omega) = \frac{(1-\varepsilon_p)\tilde{b}_c}{1-\varepsilon_p+\varepsilon_p'}\left[\frac{1}{2}\left(1-\frac{D_s}{D_{eff}}\right)\left(\frac{\tanh(\omega_{PS}^*)}{\omega_{PS}^*}\mathrm{conj}\left(\frac{\tanh(\omega_{PS}^*)}{\omega_{PS}^*}\right)\right)+\frac{D_s}{D_{eff}}\right] \tag{68}$$

$$\begin{aligned}
F_3(\omega,\omega,\omega) &= \frac{1-\varepsilon_p}{1-\varepsilon_p+\varepsilon_p'}\cosh^{-3}(\omega_{PS}^*)\times\left\{\frac{1}{4}\left(1-\frac{3D_s}{D_{eff}}\right)\left(\frac{(1-\varepsilon_p)\tilde{b}_c^2}{(1-\varepsilon_p)\tilde{a}_p+\varepsilon_p'}\left(1-\frac{2D_s}{D_{eff}}\right)+\frac{1}{2}\tilde{c}_c\right)\right.\\
&\times\left(\frac{\sinh(3\omega_{PS}^*)}{3\omega_{PS}^*}-\sinh(3\omega_{PS}^*)\frac{\tanh(\sqrt{3}\omega_{PS}^*)}{\sqrt{3}\omega_{PS}^*}\right)+\frac{1}{4}\left(3-\frac{D_s}{D_{eff}}\right)\left(\frac{(1-\varepsilon_p)\tilde{b}_c^2}{(1-\varepsilon_p)\tilde{a}_p+\varepsilon_p'}\left(1+\frac{2D_s}{D_{eff}}\right)+\frac{3}{2}\tilde{c}_c\right)\\
&\times\left(\frac{\sinh(\omega_{PS}^*)}{\omega_{PS}^*}-\sinh(\omega_{PS}^*)\frac{\tanh(\sqrt{3}\omega_{PS}^*)}{\sqrt{3}\omega_{PS}^*}\right)+\frac{(1-\varepsilon_p)\tilde{b}_c^2}{(1-\varepsilon_p)\tilde{a}_p+\varepsilon_p'}\left[\frac{D_s}{D_{eff}}\cosh^2(\omega_{PS}^*)+\left(\frac{D_s}{D_{eff}}-1\right)\sinh^2(\omega_{PS}^*)\right]\\
&\times\left[\left(2.12+4.12\frac{D_s}{D_{eff}}\right)\times\left(\frac{\sinh(2.41\omega_{PS}^*)}{2.41\omega_{PS}^*}-\cosh(2.41\omega_{PS}^*)\frac{\tanh(\sqrt{3}\omega_{PS}^*)}{\sqrt{3}\omega_{PS}^*}\right)\right.\\
&\left.-\left(2.12+0.12\frac{D_s}{D_{eff}}\right)\times\left(\frac{\sinh(0.41\omega_{PS}^*)}{0.41\omega_{PS}^*}-\cosh(0.41\omega_{PS}^*)\frac{\tanh(\sqrt{3}\omega_{PS}^*)}{\sqrt{3}\omega_{PS}^*}\right)\right]\\
&+\left(\frac{2(1-\varepsilon_p)\tilde{b}_c^2}{(1-\varepsilon_p)\tilde{a}_p+\varepsilon_p'}\left(1-\frac{2D_s}{D_{eff}}\right)+\tilde{c}_c\right)\frac{\sinh(3\omega_{PS}^*)}{12\omega_{PS}^*}+\left(3\tilde{c}_c-\frac{2(1-\varepsilon_p)\tilde{b}_c^2}{(1-\varepsilon_p)\tilde{a}_p+\varepsilon_p'}\left(1+\frac{2D_s}{D_{eff}}\right)\right)\frac{\sinh(\omega_{PS}^*)}{4\omega_{PS}^*}\\
&\left.+\frac{2(1-\varepsilon_p)\tilde{b}_c^2}{(1-\varepsilon_p)\tilde{a}_p+\varepsilon_p'}\times\left(\frac{D_s}{D_{eff}}\cosh^2(\omega_{PS}^*)+\left(\frac{D_s}{D_{eff}}-1\right)\sinh^2(\omega_{PS}^*)\right)\left(\frac{\sinh(2.41\omega_{PS}^*)}{2.41\omega_{PS}^*}+\frac{\sinh(0.41\omega_{PS}^*)}{0.41\omega_{PS}^*}\right)\right\}
\end{aligned} \tag{69}$$

where:

$$\omega_{PS}^{*} = \sqrt{j\tau_{PS}\omega} \tag{70}$$

References

Barcia, P.S., Silva, J.A.C., Rodrigues, A.E.: Adsorption equilibrium and kinetics of branched hexane isomersin pellets of BETA zeolite. Microporous Mesoporous Mater. **79**, 145–163 (2005)

Brandani, F., Ruthven, D., Co, C.G.: Measurement of adsorption equilibrium by the zero length column (ZLC) technique. Part 1: Single-component systems. Ind. Eng. Chem. Res. **42**, 1451–1461 (2003a)

Brandani, F., Ruthven, D., Co, C.G.: Measurement of adsorption equilibrium by the zero length column (ZLC) technique. Part 2: Binary systems. Ind. Eng. Chem. Res. **42**, 1462–1469 (2003b)

Brandani, S.: Effects of nonlinear equilibrium on zero length column experiments. Chem. Eng. Sci. **53**, 2791–2798 (1998)

Brandani, S., Cavalcante, C., Guimarães, A., Ruthven, D.: Heat effects in ZLC experiments. Adsorption **4**, 275–285 (1998)

Brandani, S., Jama, M., Ruthven, D.M.: ZLC measurements under nonlinear conditions. Chem. Eng. Sci. **55**, 1205–1212 (2000)

Cherntongchai, P., Brandani, S.: Liquid phase counter-diffusion measurements of aromatics in silicalite using the ZLC method. Adsorption **9**, 197–204 (2003)

Do, D.D.: Adsorption Analysis: Equilibria and Kinetics. Imperial College Press, London (1998)

Dunnewijk, J., Bosch, H., de Haan, A.B.: Adsorption kinetics of CoCl2 and PPh3 over macroreticular and gel type adsorbents by a generalized ZLC method. Chem. Eng. Sci. **61**, 4813–4826 (2006)

Eić, M., Ruthven, D.M.: A new experimental technique for measurement of intracrystalline diffusivity. Zeolites **8**, 40–45 (1988)

Eić, M., Micke, A., Kočirík, M., Jama, M., Zikánová, A.: Diffusion and immobilization mechanisms in zeolites studied by ZLC chromatography. Adsorption **8**, 15–22 (2002)

Grenier, Ph., Malka-Edery, A., Bourdin, V.: A temperature frequency response method for adsorption kinetic measurements. Adsorption **5**, 135–143 (1999)

Guiochon, G., Shirazi, S.G., Katti, A.M.: Fundamentals of Preparative and Nonlinear Chromatography. Academic Press, London (1994)

Ilić, M., Petkovska, M., Seidel-Morgenstern, A.: Nonlinear frequency response functions of a chromatographic column—A critical evaluation of their potential for estimation of single solute adsorption isotherms. Chem. Eng. Sci. **62**, 1269–1281 (2007a)

Ilić, M., Petkovska, M., Seidel-Morgenstern, A.: Nonlinear frequency response method for estimation of single solute adsorption isotherms. Part I. Theoretical basis and simulations. Chem. Eng. Sci. **62**, 4379–4393 (2007b)

Ilić, M., Petkovska, M., Seidel-Morgenstern, A.: Nonlinear frequency response method for estimation of single solute adsorption isotherms. Part II. Experimental study. Chem. Eng. Sci. **62**, 4394–4408 (2007c)

Kärger, J., Ruthven, D.M.: Diffusion in Zeolites and Other Microporous Solids. Wiley, New York (1992)

Naphtali, L.M., Polinski, L.M.: A novel technique for characterisation of adsorption rates on heterogeneous surfaces. J. Phys. Chem. **67**, 369–375 (1963)

Park, I.S., Petkovska, M., Do, D.D.: Frequency response of an adsorber with the modulation of the inlet molar flow-rate: Part. I. A semi-batch adsorber, Chem. Eng. Sci. **53**, 819–832 (1998)

Petkovska, M.: Non-linear frequency response of non-isothermal adsorption controlled by micropore diffusion with variable diffusivity. J. Serb. Chem. Soc. **65**, 939–961 (2000)

Petkovska, M.: Nonlinear frequency response of nonisothermal adsorption systems. Nonlinear Dyn. **26**, 351–370 (2001)

Petkovska, M.: Application of nonlinear frequency response to adsorption systems with complex kinetic mechanisms. Adsorption **11**, 497–502 (2005a)

Petkovska, M.: Nonlinear frequency response method for investigation of equilibria and kinetics in adsorption systems. In: Spasic, A.M., Hsu, J.P. (eds.) Finely Dispersed Particles: Micro, Nano- and Atto-Engineering, pp. 283–327. CRC, Taylor & Francis, Boca Raton (2005b)

Petkovska, M., Do, D.D.: Nonlinear frequency response of adsorption systems: isothermal batch and continuous flow adsorber. Chem. Eng. Sci. **53**, 3081–3097 (1998)

Petkovska, M., Do, D.D.: Use of higher order FRFs for identification of nonlinear adsorption kinetics: single mechanisms under isothermal conditions. Nonlinear Dyn. **21**, 353–376 (2000)

Petkovska, M., Petkovska, L.T.: Use of nonlinear frequency response for discriminating adsorption kinetics mechanisms resulting with bimodal characteristic functions. Adsorption **9**, 133–142 (2003)

Petkovska, M., Seidel-Morgenstern, A.: Nonlinear frequency response of a chromatographic column. Part I: Application to estimation of adsorption isotherms with inflection points. Chem. Eng. Commun. **192**, 1300–1333 (2005)

Rees, L.V.C., Song, L.: Frequency response methods for the characterization of microporous solids. In: Kamellopoulos, N.K. (ed.) Recent Advances in Gas Separation by Microporous Ceramic Membranes, pp. 139–186. Elsevier, Amsterdam (2000)

Rouquerol, F., Rouquerol, J., Sing, K.: Adsorption by Powders and Porous Solids. Academic Press, London (1999)

Ruthven, D.M., Brandani, S.: Measurement of diffusion in porous solids by ZLC methods. In: Kamellopoulos, N.K. (ed.) Recent Advances in Gas Separation by Microporous Ceramic Membranes, pp. 187–212. Elsevier, Amsterdam (2000)

Seidel-Morgenstern, A.: Experimental determination of single solute and competitive adsorption isotherms—Review. J. Chromatogr. A **1037**, 255–272 (2004)

Song, L., Rees, L.V.C.: Frequency response diffusion of propane in Silicalite 1. Microporous Mater. **6**, 363–374 (1996)

Vinh-Thang, H., Huang, Q., Ungureanu, A., Eić, M., Trong-On, D., Kaliaguine, S.: Structural and diffusion characterizations of steam-stable mesostructured zeolitic UL-ZSM-5 materials. Langmuir **22**, 4777–4786 (2006)

Wang, Y., LeVan, M.D.: Mixture diffusion in nanoporous adsorbents: development of Fickian flux relationship and concentration-swing frequency response method. Ind. Eng. Chem. Res. **46**, 2141–2154 (2007)

Wang, Y., Sward, B.K., LeVan, M.D.: New frequency response method for measuring adsorption rates via pressure modulation: application to oxygen and nitrogen in a carbon molecular sieve. Ind. Eng. Chem. Res. **42**, 4213–4222 (2003)

Weiner, D.D., Spina, J.F.: Sinusoidal Analysis and Modelling of Weakly Nonlinear Circuits. Reinhold, New York (1980)

Yasuda, Y.: Determination of vapor diffusion coefficients in zeolite by the frequency response method. J. Phys. Chem. **86**, 1913–1917 (1982)